

First detection of solar neutrinos from the CNO cycle with Borexino

Gioacchino Ranucci
INFN - Milano

On behalf of the Borexino
Collaboration



June 23, 2020

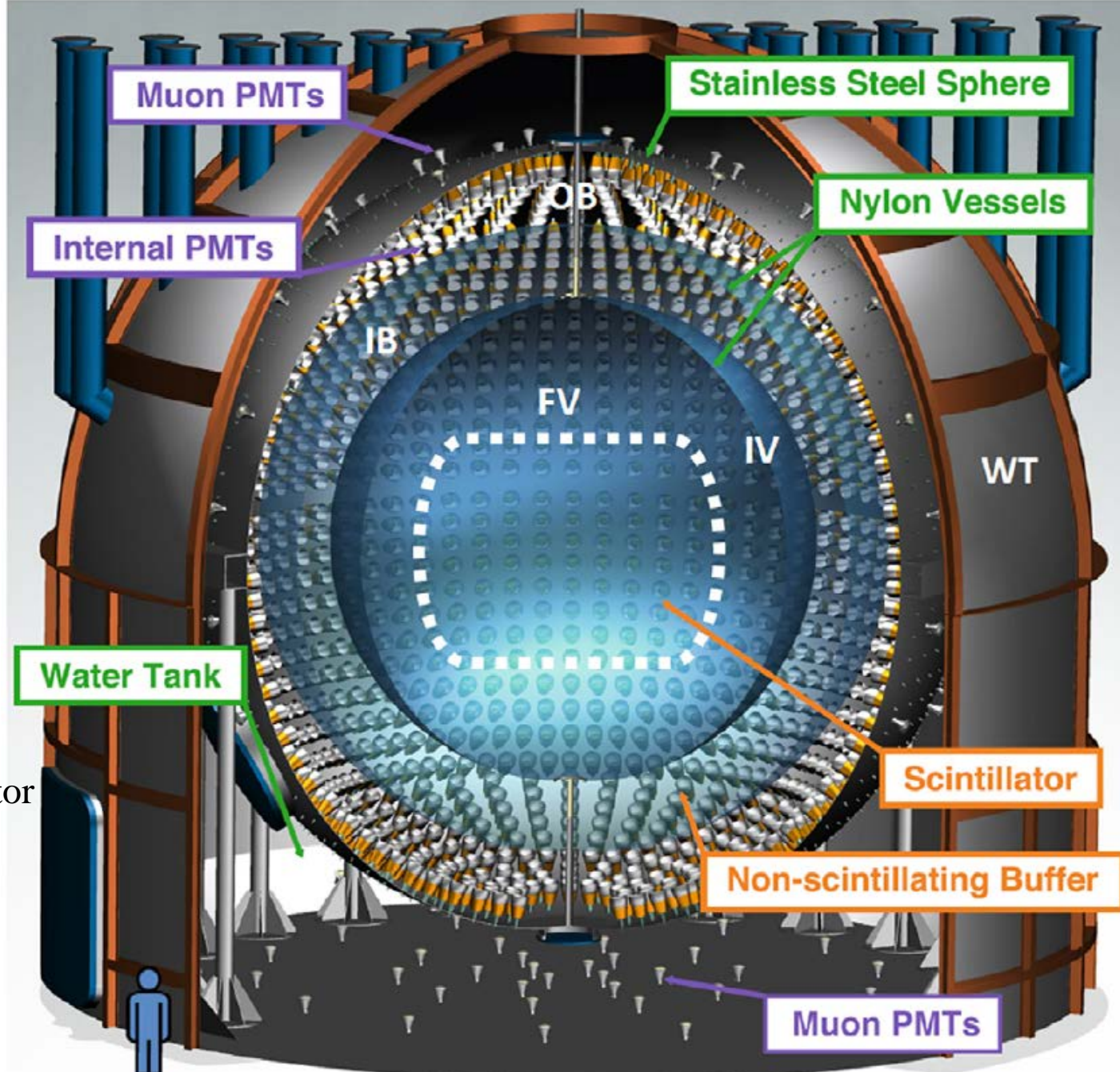
The Borexino detector @ Gran Sasso

Active
volume 280
tons of liquid
scintillator

Detection principle

$$\nu_x + e \rightarrow \nu_x + e$$

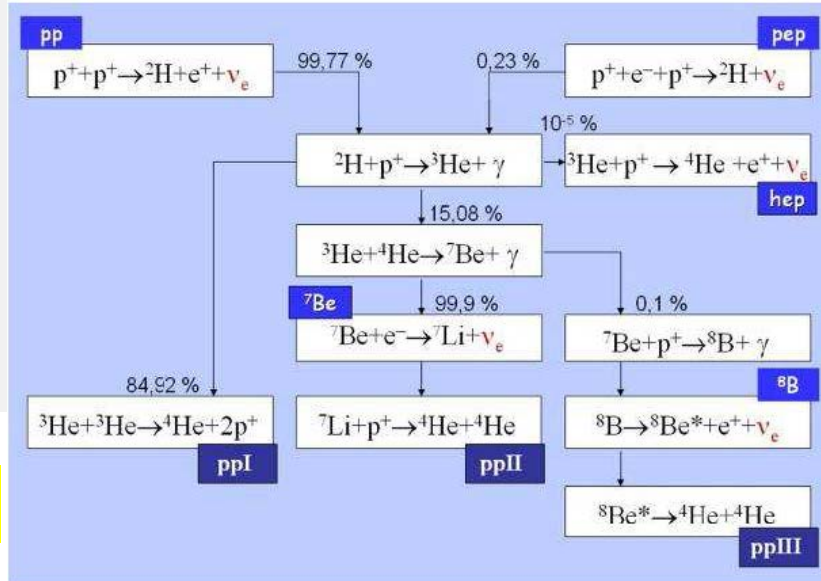
Elastic scattering off the
electrons of the scintillator
threshold at ~ 60 keV
(electron energy)



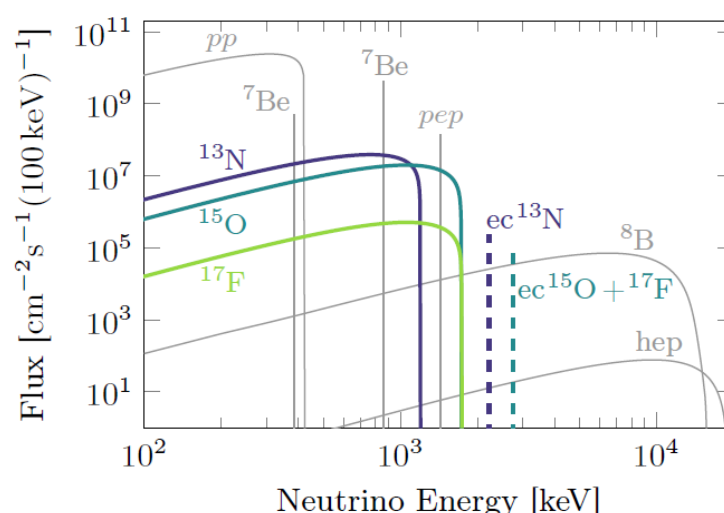
Standard Solar Model : “engine” of the Sun, solar neutrinos production and spectrum predictions

Developed by John Bahcall for more than 40 years

pp chain

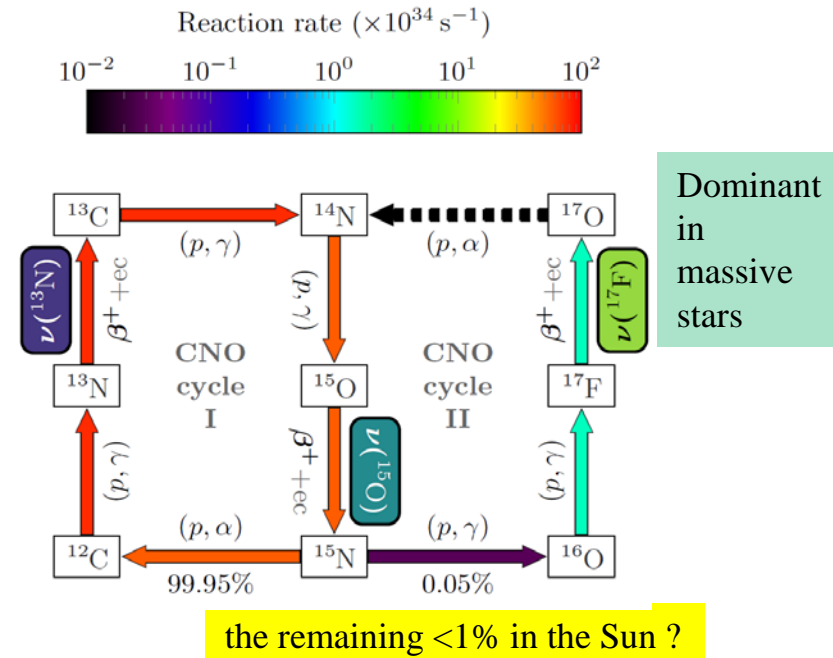


Latest SSM spectral prediction
A. Serenelli
 EPJA, volume 5, id 78 (2016)
N. Vinyoles et al.
 The Astrophysical Journal, 835:202 (16pp), 2017



2020 Jun 23

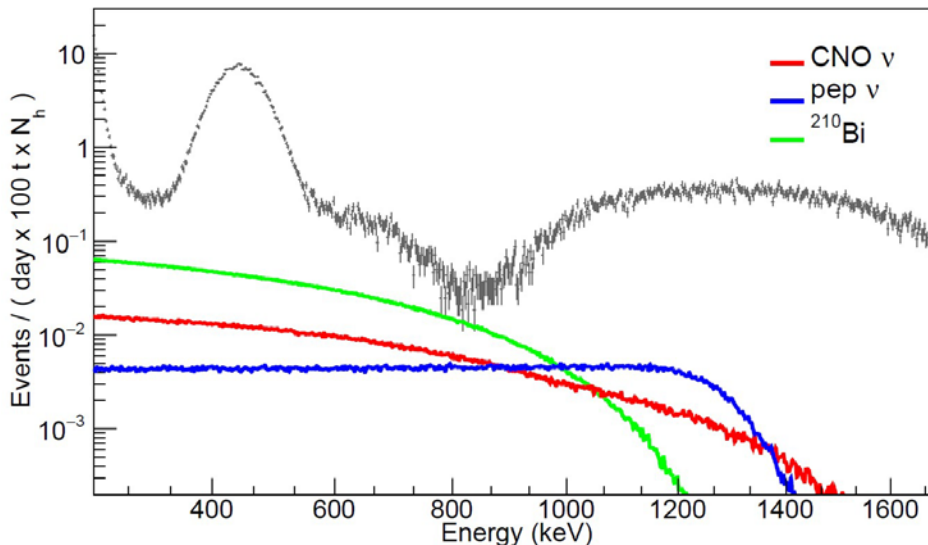
G. Ranucci - First detection of solar neutrinos from CNO cycle with Borexino



Controversy about the surface metallicity composition of the Sun: predictions differ up to 28% for the CNO ν flux using lower (LZ) or higher Z (HZ) models

The Borexino quest for CNO neutrinos after the complete pp chain measurement

CNO ν – pep ν – ^{210}Bi correlations



- Borexino data
- CNO ν expected spectrum
- ^{210}Bi spectrum
- pep ν spectrum

The **spectral fit** returns only the sum of CNO and ^{210}Bi , if both are left free

Note also the low rates:

- $R(\text{CNO } \nu)_{\text{expected}} \sim 3\text{-}5 \text{ cpd}/100\text{ton}$
- $R(^{210}\text{Bi}) \sim 10 \text{ cpd}/100\text{ton}$
- $R(\text{pep}) \sim 2.5 \text{ cpd}/100\text{ton}$

Thanks to Borexino unprecedented purity
@ 95% C.L. $^{232}\text{Th} < 5.7 \cdot 10^{-19} \text{ g/g}$ $^{238}\text{U} < 9.4 \cdot 10^{-20} \text{ g/g}$
other backgrounds less relevant apart the cosmogenic ^{11}C

The pep flux can be constrained at the 1.4 % level through the solar luminosity constraint coupled to SSM predictions on the pp to pep rate ratio and the most recent oscillation parameters - J. Bergström et al., JHEP, 2016:132, 2016

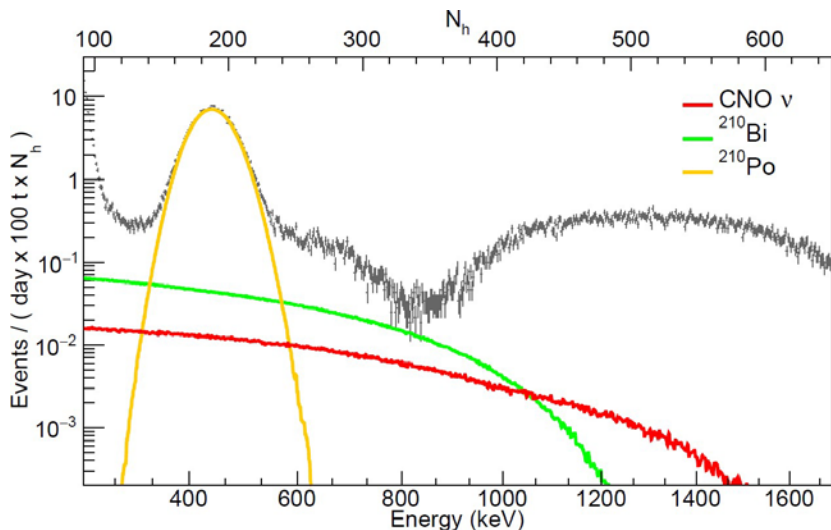
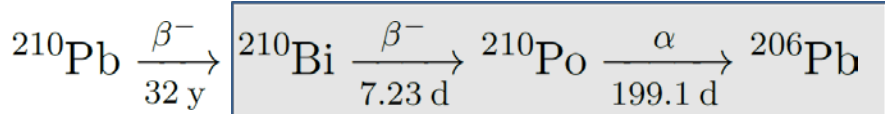
^{210}Bi independent determination from ^{210}Po

Degeneracy in the fit removable with a constraint on ^{210}Bi

Independent estimation of ^{210}Bi rate

^{210}Bi - ^{210}Po analysis:

Extract the ^{210}Bi decay rate in Borexino through the study of the ^{210}Po decay rate



^{210}Po is “easier” to identify wrt ^{210}Bi :

- Monoenergetic decay \rightarrow “gaussian” peak
- α decay \rightarrow pulse shape discrimination

If the ^{210}Bi is in equilibrium with ^{210}Po , an independent measurement of the latter decay rate gives directly the ^{210}Bi one (secular equilibrium scenario)

→ The quest for CNO is turned into the quest of ^{210}Bi through ^{210}Po !

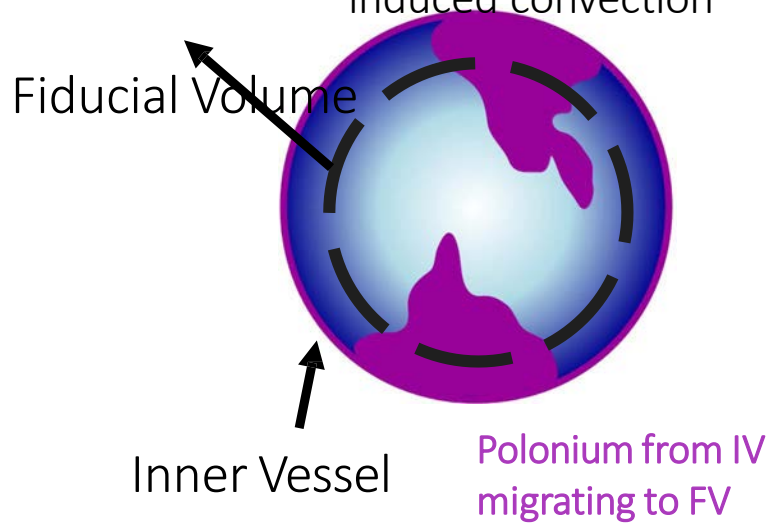
Posters: “Strategy of detection of solar CNO neutrinos with Borexino Phase-III data” Xuefeng Ding #438 session 2

“Borexino Sensitivity Studies towards Detection of Solar Neutrinos from the CNO Fusion Cycle” Ömer Penek #235 session 3

2020 Jun 23

Hurdle - diffusion and convection of ^{210}Po from the vessel surface

^{210}Po moves from the vessel surface into the scintillator and within the scintillator itself → getting moved by diffusion and temperature induced convection



Pure exponential decay ($t_{1/2} = 138.4$ days) to the intrinsic value is perturbed by the presence of strong convective motions (purple blobs), caused mostly by seasonal and man-made temperature change in the experimental Hall

$$\partial_t \rho(r) = D \nabla^2 \rho(r) - \frac{\rho(r)}{\tau_{\text{Po}}} \rightarrow \rho(r) = \rho_0 \frac{\sinh(r/\lambda)}{r/\lambda}$$

Diffusion length in PC
 $\lambda = \sqrt{D \tau_{\text{Po}}} \approx 20 \text{ cm}$

Even tiny amount of ^{210}Pb – source of ^{210}Po – present on vessel surface are relevant at the Borexino extreme radiopurity level

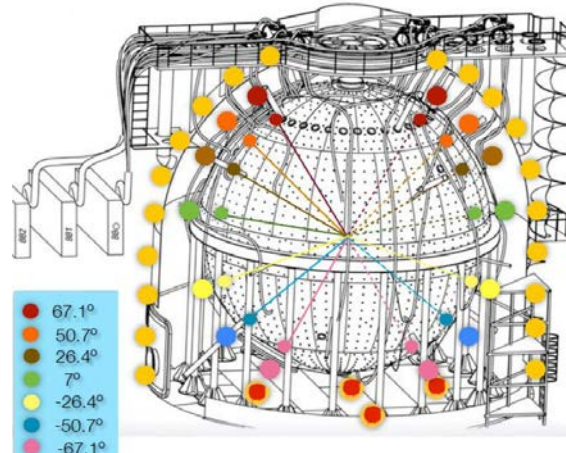
without taking compensating measures convection is dominant

Multiple approaches to monitor, understand, and suppress the temperature variations

Thermal insulation &
Active Gradient
Stabilization System



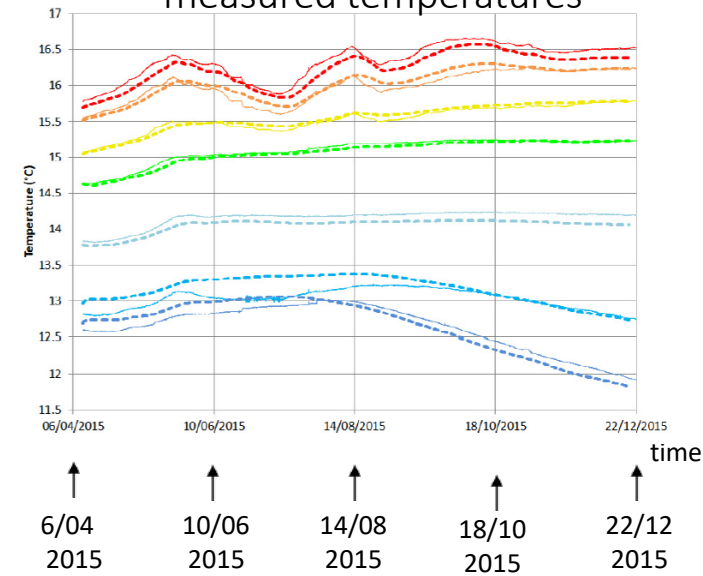
Temperature monitoring probes



54 temperature probes

Fluid dynamical simulation

Very good agreement with
measured temperatures

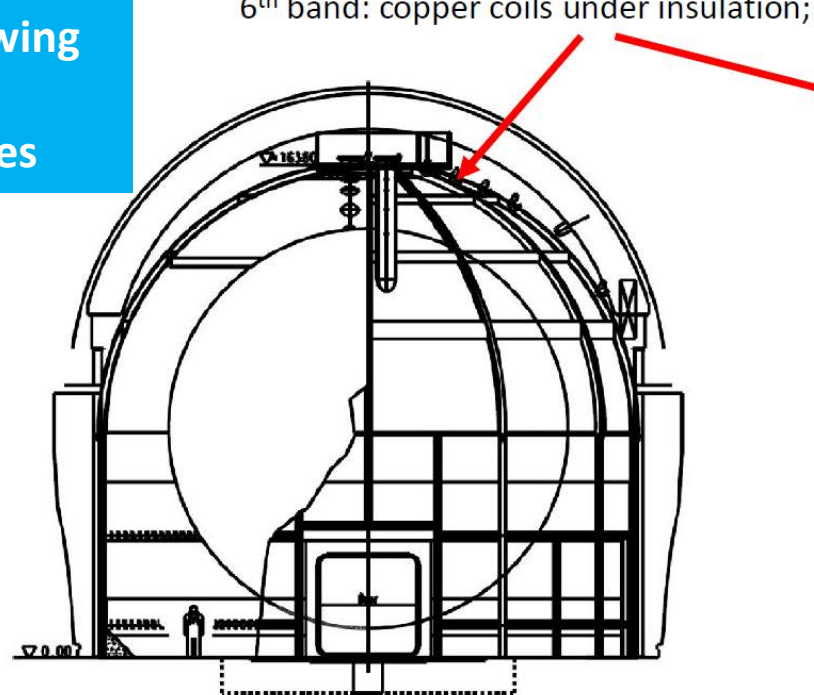


- Double layer of mineral wool (thermal conductivity down to 0.03 W/m/K) & Active Gradient Stabilization System (2014-2016)
- Temperature Probes (2014-2015)
- Fluid dynamical simulations
- Hall C Temperature Stabilization (2019)

V. di Marcello et al., NIM A 964, id. 163801

Top-Bottom gradient and active temperature control system

Controlled
temperature
water flowing
in copper
serpentines



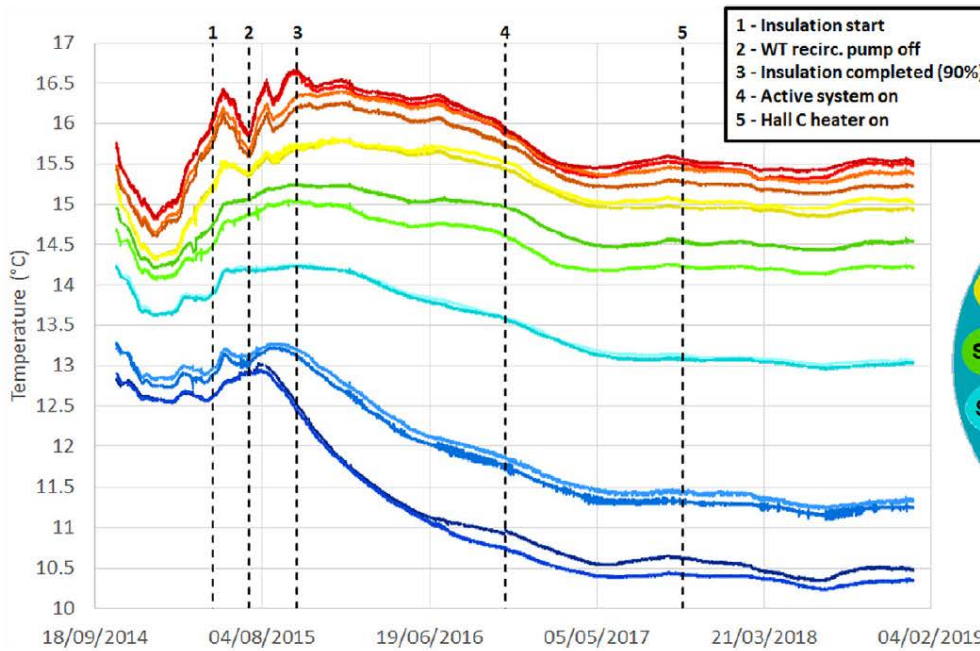
Poster
“Temperature
Stabilization of
the BOREXINO
Detector for
the CNO
Quest”
Aldo Ianni and
Nicola Rossi
#297 session 4

Key to ensuring a static liquid condition was the establishment of a stable top-bottom temperature gradient

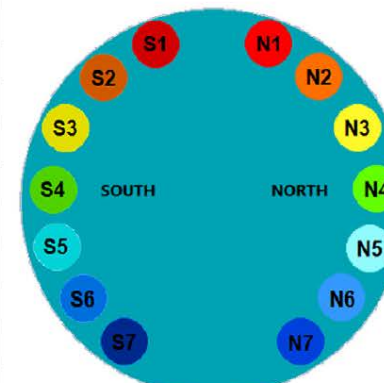
The bottom temperature was established by the rock temperature

The water in the serpentines controls the top temperature → **top-bottom gradient stabilized**

Temperature evolution from the probes



Global view of stabilization from 2015

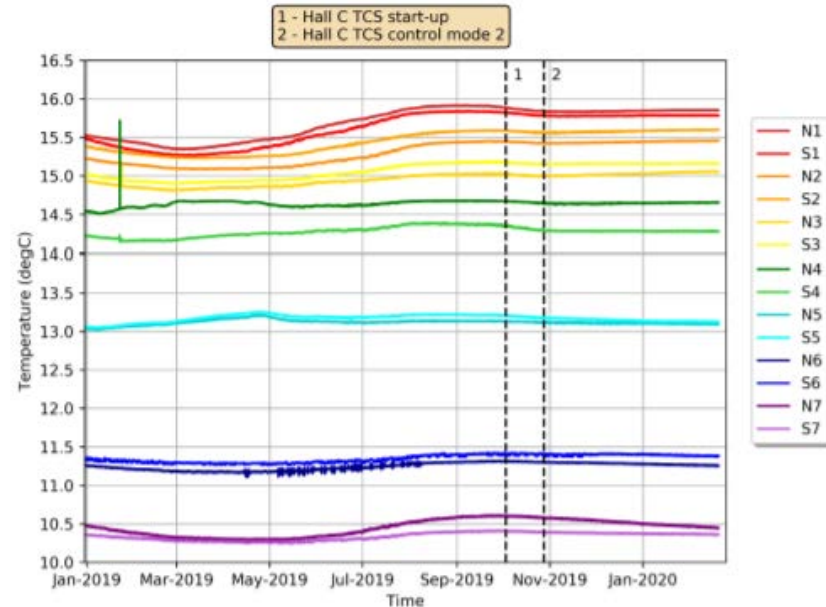


Probes sensing
the outer buffer

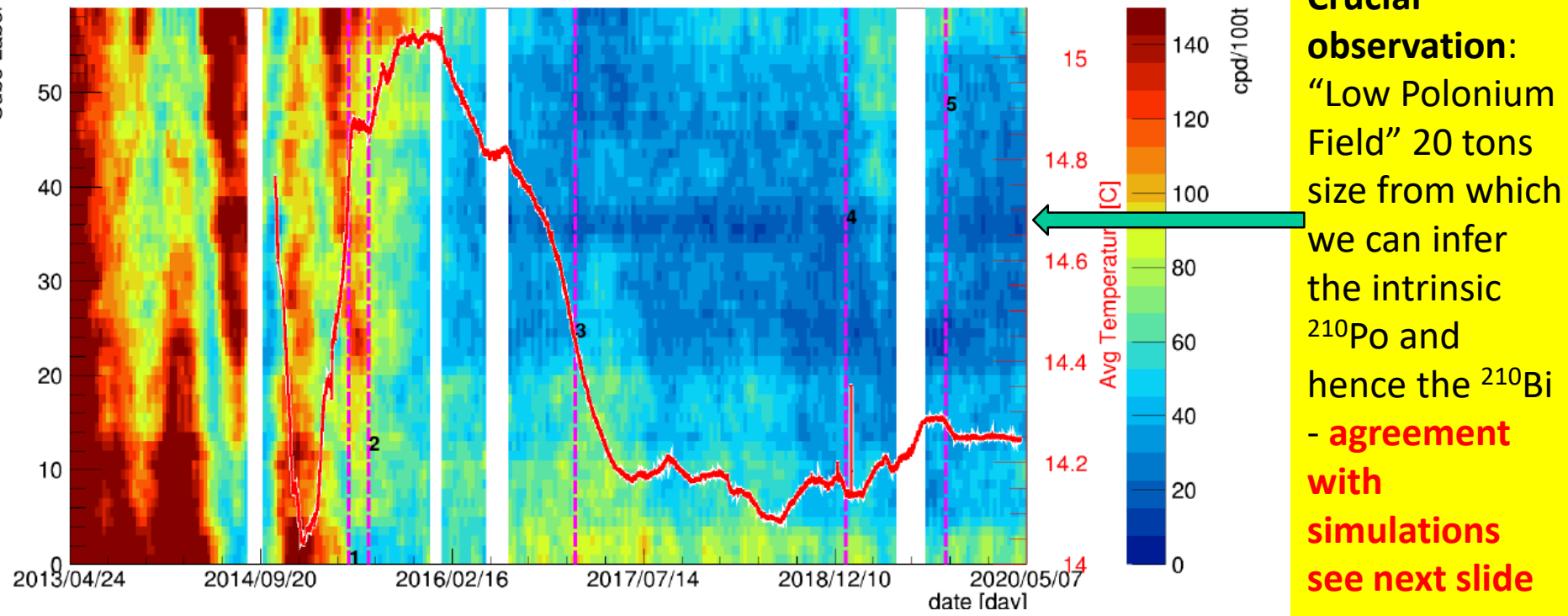
Snapshot of the last year

Achieved excellent temperature stability with the establishment of a clear temperature gradient

Probes resolution $0.07\ ^{\circ}\text{C}$



A 2D detailed view - Polonium data spatial mapping vs. time



Convective condition before insulation

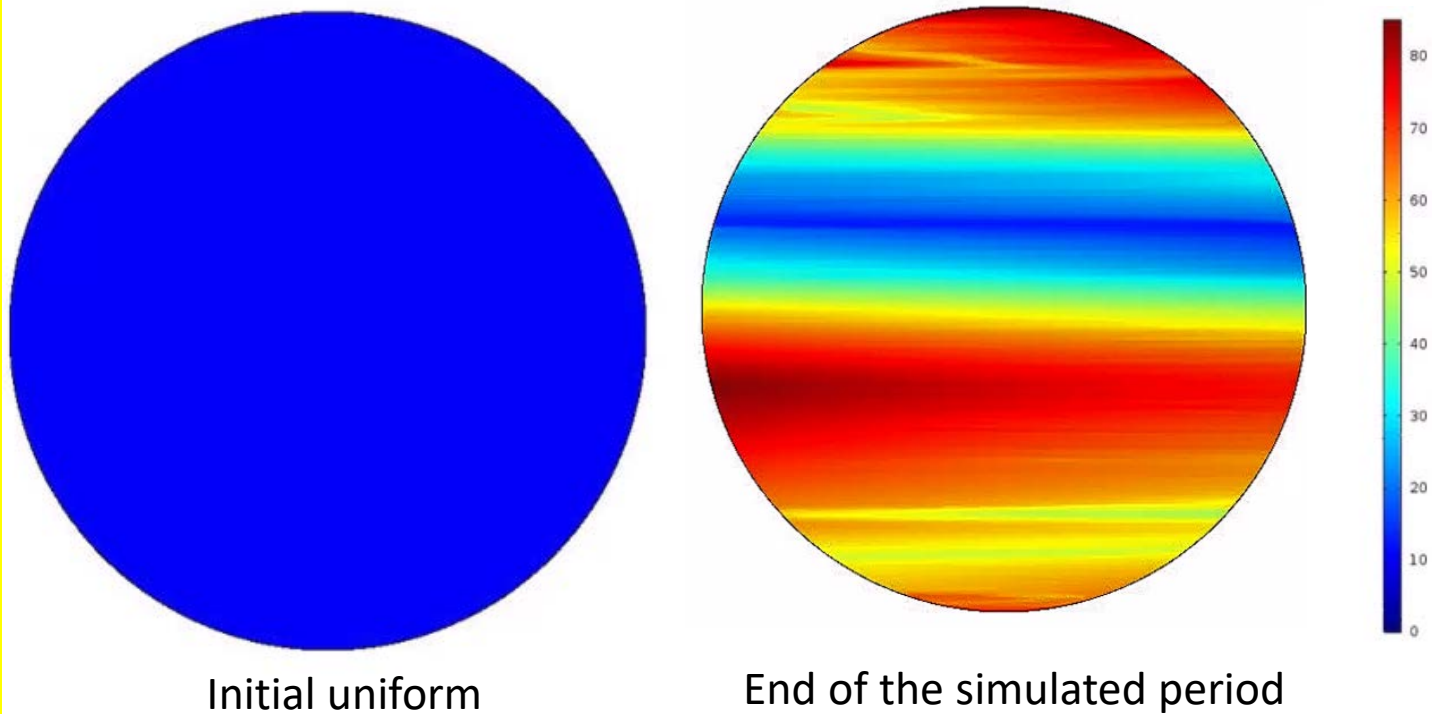
Quiet situation after insulation

Stabilization measures were very effective at reducing the ^{210}Po motion

1. Beginning of the Insulation Program
2. Turning off the water recirculation system in the Water Tank
3. Start of the active temperature control system operations
4. Change of the active control set points
5. Installation and commissioning of the Hall C temperature control system.

Prediction of ^{210}Po volumetric pattern – Fluid dynamical simulation with the insulation cover of the Water Tank and the measured temperature profiles

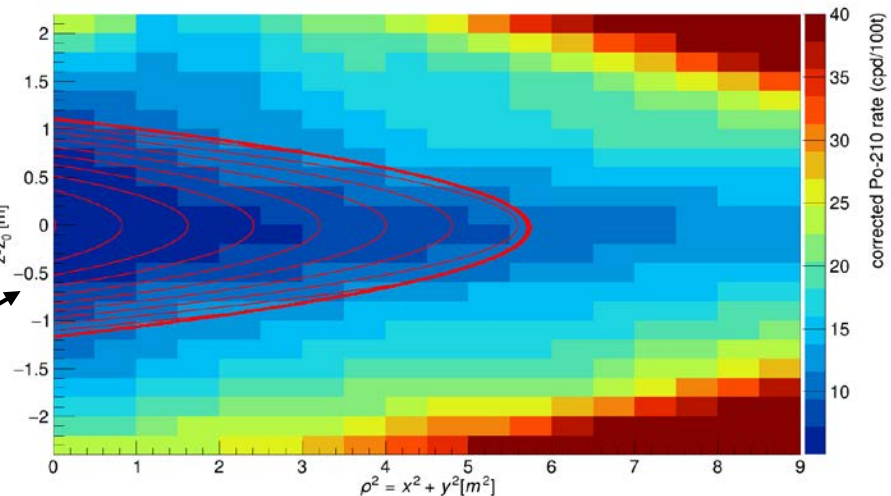
^{210}Po rate vs. time within the vessel (initial condition and final solution displayed) taking into account a surface distribution on the wall of the vessel. The simulation describes the migration due to the residual convective motion post-insulation



Predicted more residual “turbulence” (and hence Polonium) in the bottom and the dynamical formation of a “minimum” ^{210}Po region above the equator, unaffected by the ^{210}Po influx from the surface

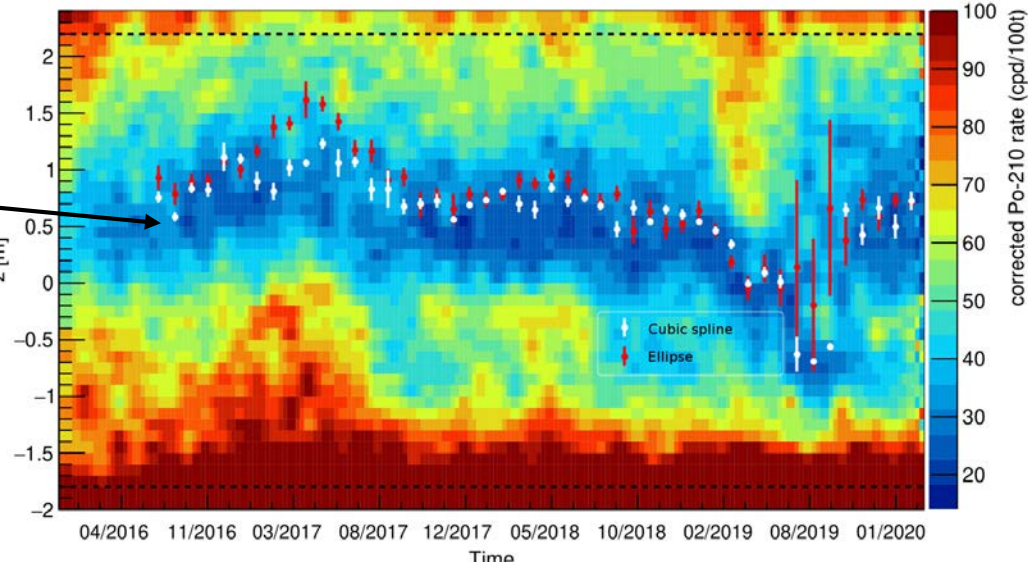
^{210}Bi upper limit from ^{210}Po data

- ^{210}Po (alpha) events are fitted to find the minimum ^{210}Po rate in the sub-region



Distribution of ^{210}Po events in the blindly aligned data-set

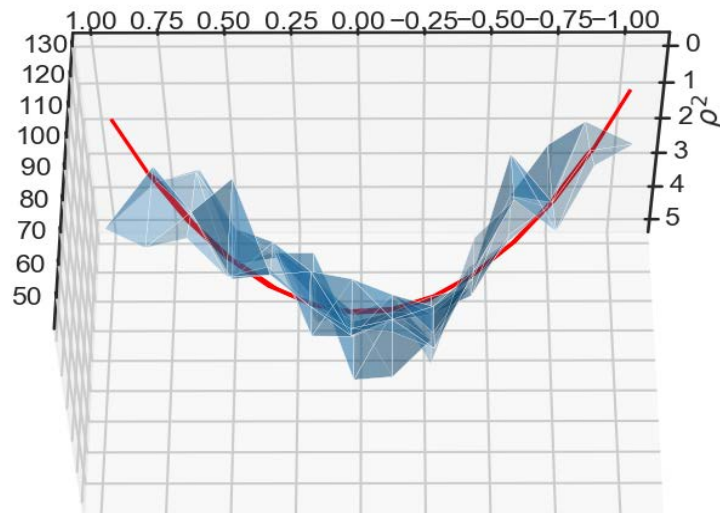
- “Aligning” the data:
 1. Fit paraboloid/spline over monthly data
 2. Extract z-position (z_0) over time
 3. Create “aligned” dataset where each data point is shifted with the z_0 from the previous month. This reduces bias in the final result.



Reconstructed central position of LPoF over time for different methods

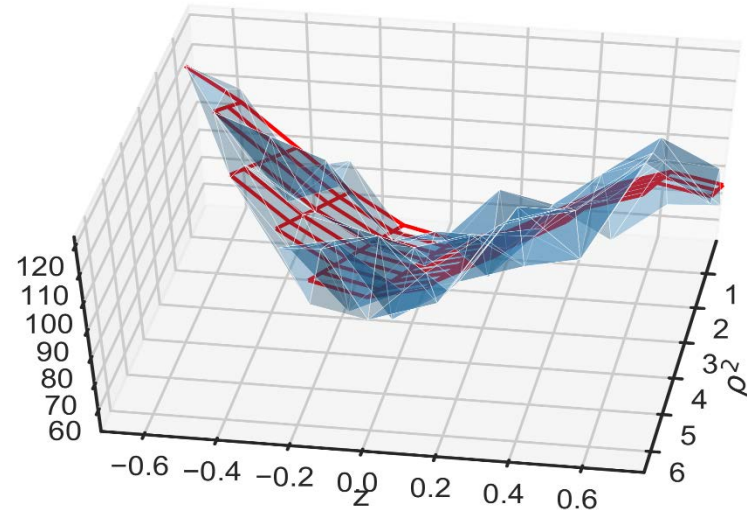
Fitting the aligned ^{210}Po data

Paraboloid



$$R_{Po} = R_{min} \epsilon \cdot \left(1 + \frac{\rho^2}{a^2} + \frac{(z - z_0)^2}{b^2} \right) + R_\beta$$

Spline fit:



Account for complexity along the z axis with a cubic spline model using a Bayesian nested sampling algorithm

Both methods agree within systematics:

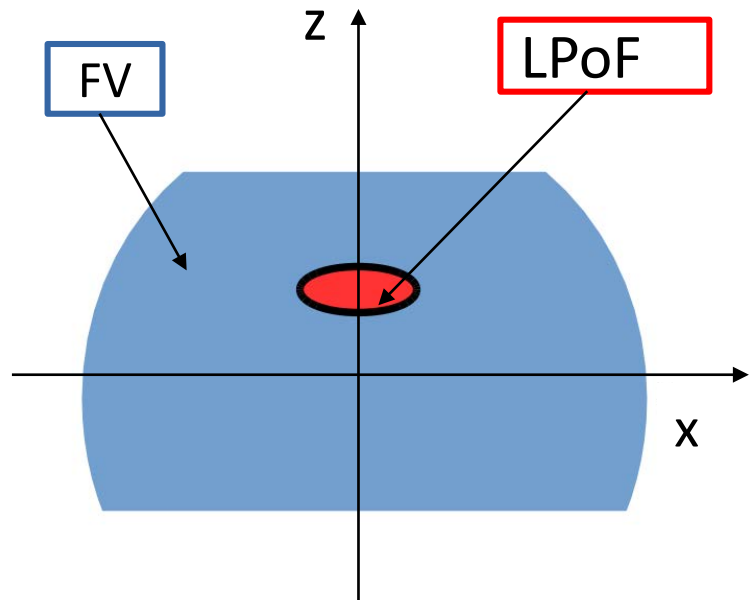
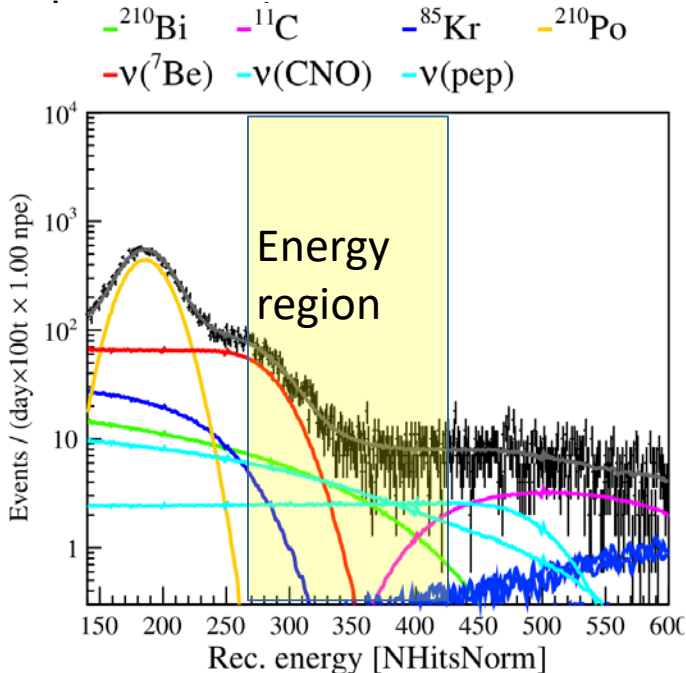
R_{min} (cpd/100t)	σ_{fit}	σ_{mass}	$\sigma_{binning}$	$\sigma_{^{210}\text{Bi homog.}}$	$\sigma_{\beta \text{ leak}}$	σ_{Total}
11.5	0.88	0.36	0.31	See next slides	0.30	See next slides

^{210}Bi spatial uniformity systematics

^{210}Bi constraint based on 20t region analysis

→ CNO analysis: implicitly extrapolating the ^{210}Bi constraint from the LPoF to the larger FV mass (70t)

Precision level we state ^{210}Bi uniformity in the FV?" → systematic to the ^{210}Bi spatial



Analyzing β spatial distribution of events in a large energy range ($0.554 \text{ MeV} < E < 0.904 \text{ MeV}$)

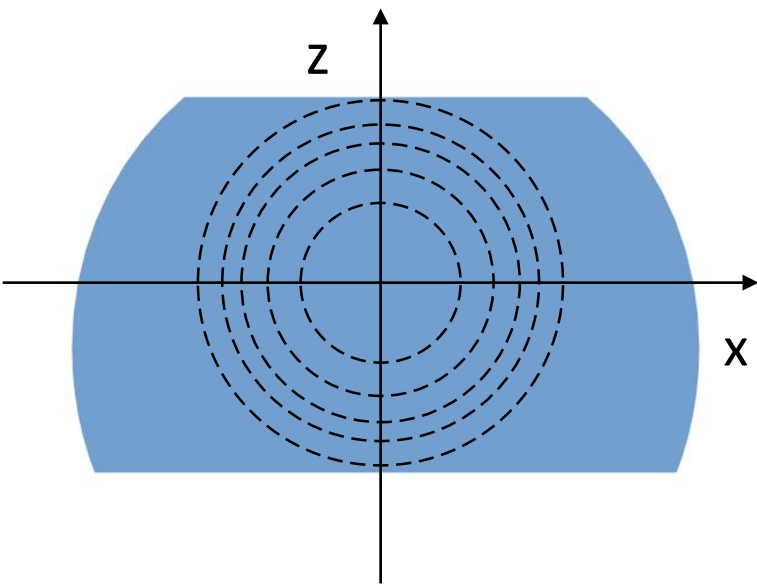
- ~75% neutrinos
- ~15% ^{210}Bi
- ~10% ^{11}C and ^{85}Kr

Rate variations are attributed to ^{210}Bi events (conservative approach)

^{210}Bi spatial uniformity systematics

Radial β analysis

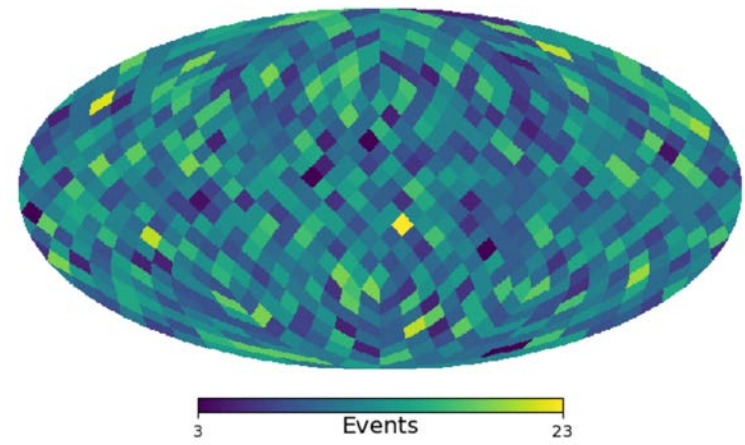
Radial shells



0.51 cpd/100t

Angular β analysis

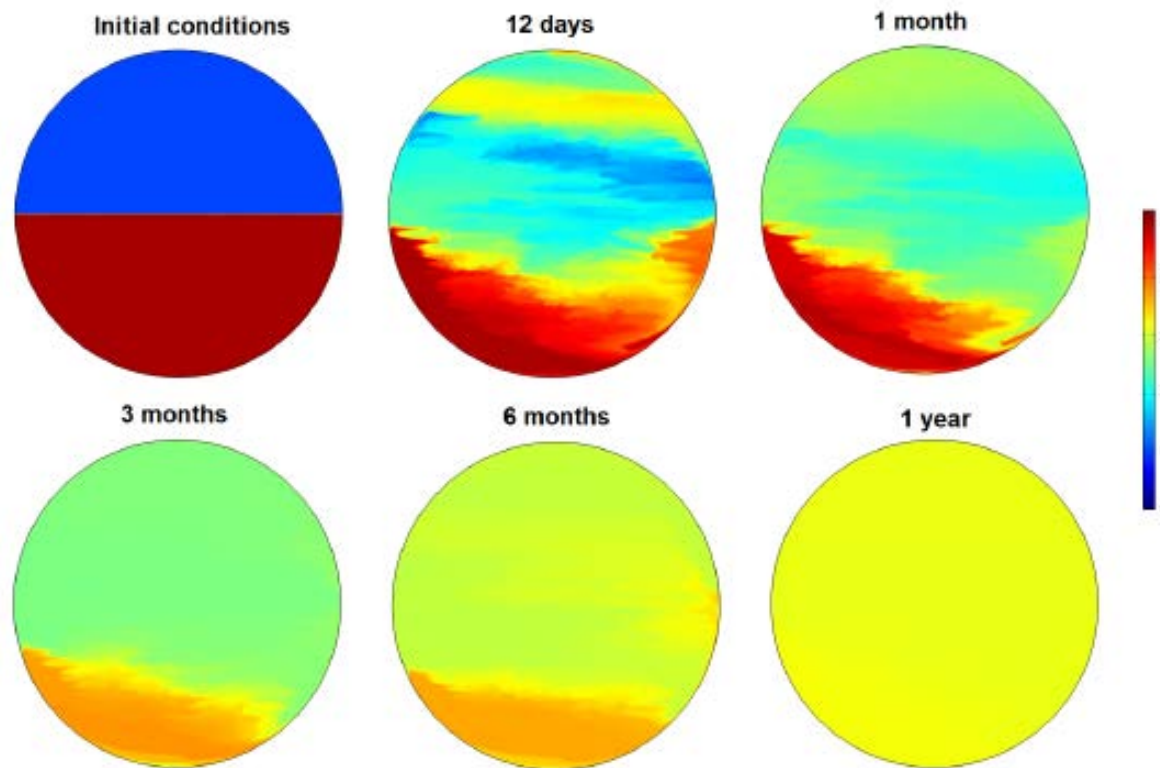
Spherical harmonics decomposition



0.59 cpd/100t

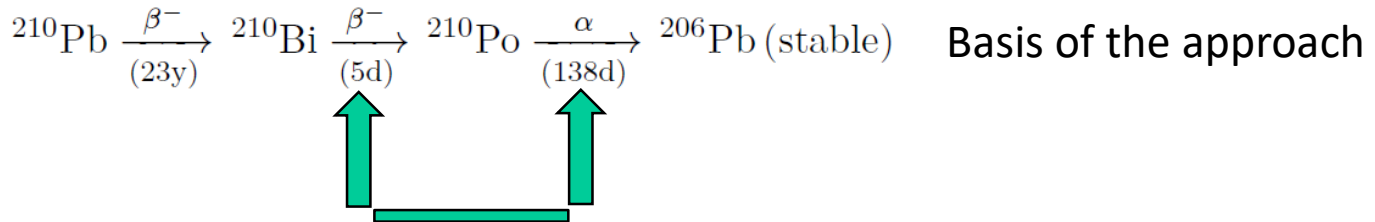
Overall ^{210}Bi spatial uniformity systematics: 0.78 cpd/100t

Simulation of the $^{210}\text{Pb}/^{210}\text{Bi}$ uniformity



Evolution of an initial non uniform $^{210}\text{Pb}/^{210}\text{Bi}$ distribution pre-insulation and with the experimental temperature distributions at that time → **uniformity** reached in 1 year in the entire inner vessel

^{210}Po and ^{210}Bi final numerical assessment



^{210}Po rate inferred from the Low Polonium Field with all errors

$R_{min}(\text{cpd}/100t)$	σ_{fit}	σ_{mass}	$\sigma_{binning}$	$\sigma_{^{210}\text{Bi homog.}}$	$\sigma_{\beta \text{ leak}}$	σ_{Total}
11.5	0.88	0.36	0.31	0.78	0.30	1.3

The ^{210}Po evaluated rate still possibly contaminated with residual ^{210}Po from the vessel surface → upper limit to the rate of ^{210}Bi

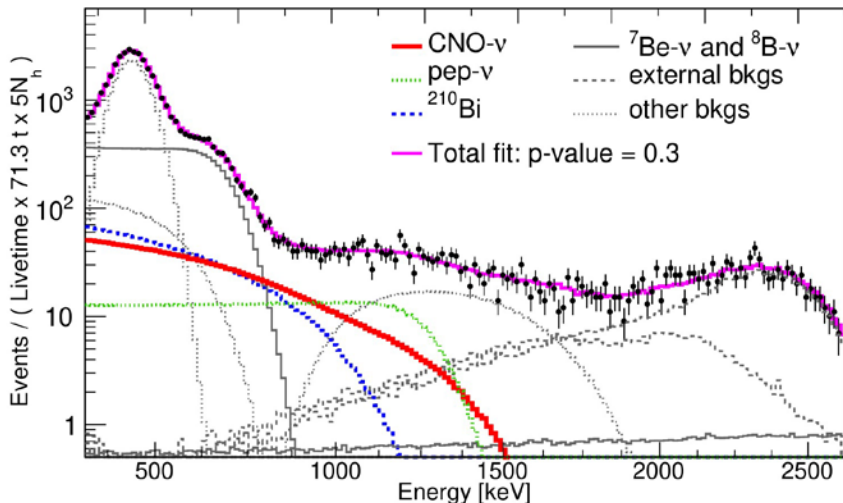
$$\boxed{R(^{210}\text{Bi}) \leq 11.5 \pm 1.3 \text{ cpd}/100t}$$

Sought constraint essential to break the degeneracy with CNO →
Outcome of the relentless years-long effort to stabilize the detector
and understand the ^{210}Po behavior in the Inner Vessel

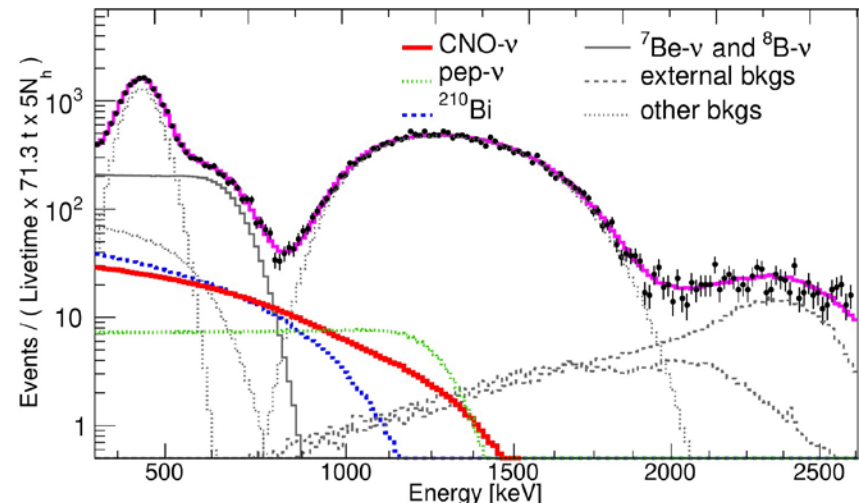
Poster: "Extraction of ^{210}Bi via ^{210}Po for CNO neutrino detection with Borexino" Sindhujha Kumaran, Davide Basilico, Xuefeng Ding and Alexandre Göttel #212 session 3

CNO- ν analysis: Phase-III MV fit

TFC-subtracted spectrum



TFC-tagged spectrum



Multivariate fit (0.32-2.64 MeV)
July '16 – February '20

Maximization of a binned likelihood **3 distributions simultaneously**:

- Reconstructed energy for TFC-tagged and TFC-subtracted datasets (^{11}C identification)
- Radial position

pep-ν rate constrained
 ^{210}Bi rate constrained
CNO rate
 Other ν and bkg rates

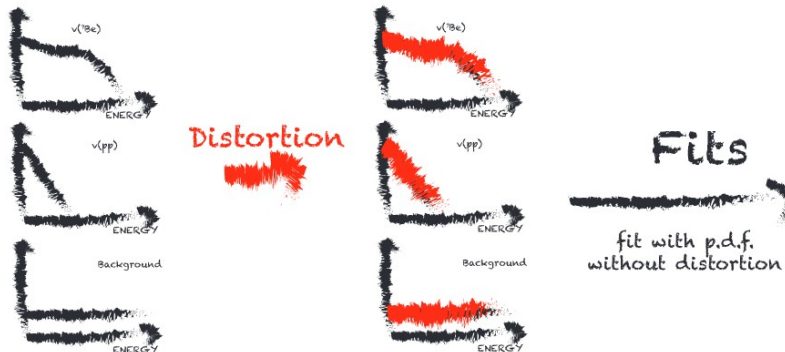
→ solar luminosity constraint
 → ^{210}Bi - ^{210}Po tagging
 → free to vary
 → free to vary

Result

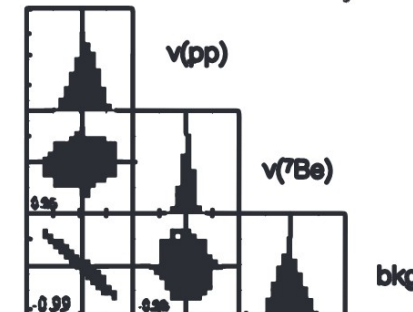
CNO best fit 7.2 cpd/100t
asymmetric confidence interval -1.7 +2.9 cpd/100t
(stat only) asymmetry \leftrightarrow ^{210}Bi upper limit

Systematic sources and final CNO-v result

Monte Carlo → simulate distorted datasets,
fit with un-distorted PDFs



Look at the width
→ Get $\sigma_{\text{stat}}^{\text{expected}}$
and σ_{sys}



1) Fit conditions
→ negligible

2) ^{11}C spectrum
deformation by noise cuts

3) Energy response function: energy scale (~0.23%),
non-uniformity (~0.28%), non-linearity (~0.4%) from
detector calibration

4) ^{210}Bi spectral
shape (diff.~18%)

Final syst:
-0.5 +0.6
cpd/100t

Final CNO result **7.2 (-1.7 +3.0)** cpd/100t stat + sys

corresponding to a flux of neutrinos on
Earth of **$7.0 (-1.9 +2.9) \times 10^8 \text{ cm}^{-2} \text{ s}^{-1}$**

Significance of CNO-v detection

Likelihood ratio test

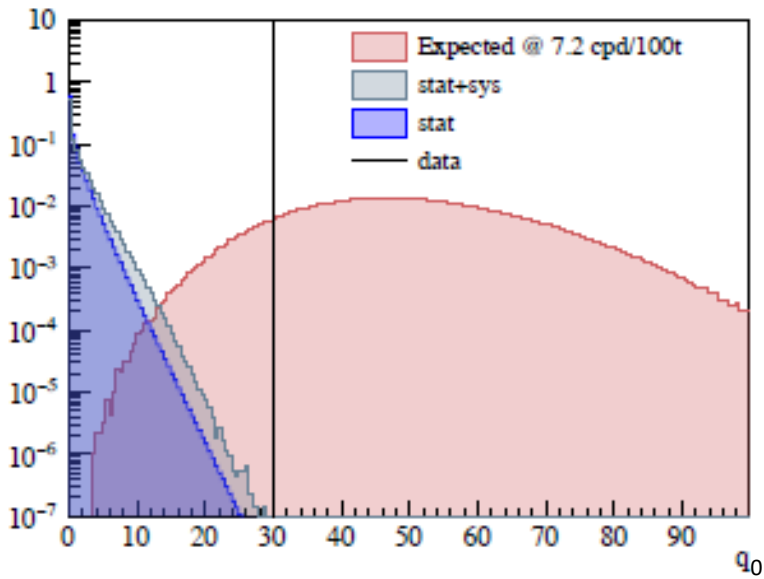
Determination of the q_0 discovery test statistic from the likelihood with and without the CNO signal

G. Cowan et al., Eur. Phys. J. C, 71:1554, 2011

13.8 millions pseudo-datasets
with deformed PDFs and no
CNO to determine the q_0
reference distribution

$q_0(\text{data})$ from the real dataset

From the MC distributions **p-value** of q_0 (grey curve) with respect to q_0 (data) (black line) → correspondingly **significance** greater than **5σ** at 99% CL
Consistent with **5.1σ** through the log-likelihood from the fit folded with uncertainties



No CNO hypothesis disfavored at **5σ**

With these results Borexino marks the
first detection ever of CNO solar neutrinos

Posters: "Spectral fit of Borexino Phase-III data for the detection of CNO solar neutrinos" Zara Bagdasarian, Davide Basilico, Giulio Settanta #238 session 2

"The Borexino Monte Carlo simulations for the CNO neutrino detection" Davide Basilico #181 session 2

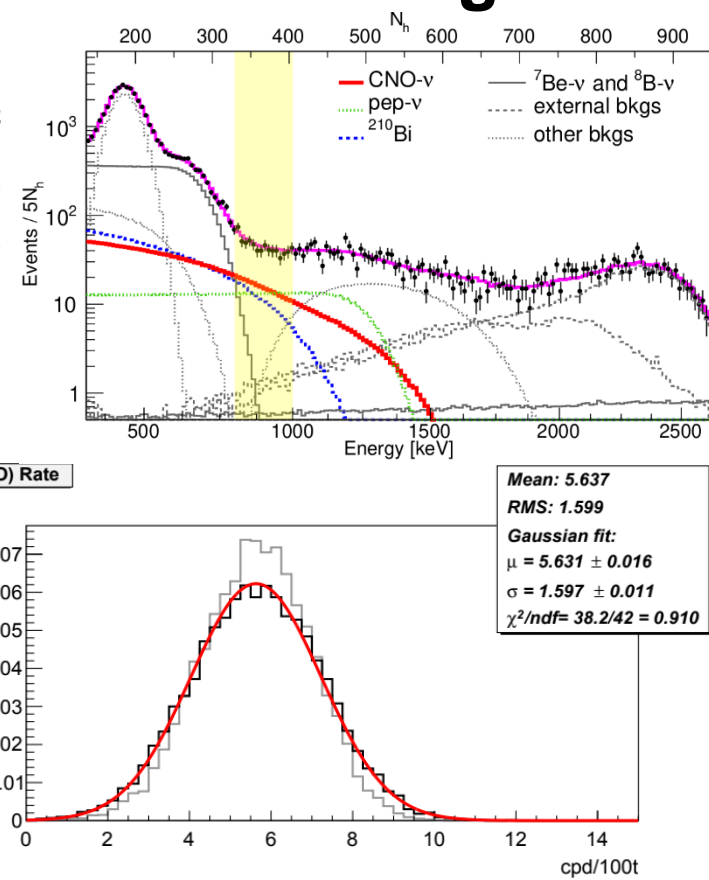
Result corroborated by a simplified Counting Analysis

We perform a counting analysis in a Region of Interest (ROI) determined maximizing a S/B Figure of Merit and using an analytical modeling of the detector response.

Species (S_i)	Events	Fraction
N	823 ± 28.7	
^{210}Bi	261.5 ± 29.6	0.31
$\nu(\text{pep})$	171.7 ± 2.4	0.21
$\nu(^7\text{Be})$	86.8 ± 2.6	0.10
^{11}C	57.9 ± 5.8	0.07
Others	15.6 ± 1.6	0.02
$\sum_i S_i$	593.5 ± 30.4	0.71
$N - \sum_i S_i$	229.5 ± 41.8	0.29

Number of expected events of ^{210}Bi and pep neutrinos in the ROI is calculated according to the same bounds used in the MV fit

For the other species we use a reference response model of the detector



Systematics are obtained as the width of the distribution of the CNO rate after varying parameters on 10^4 Toy-MC realizations where we determine the number of CNO events by subtracting all the other species from the total events in the ROI.

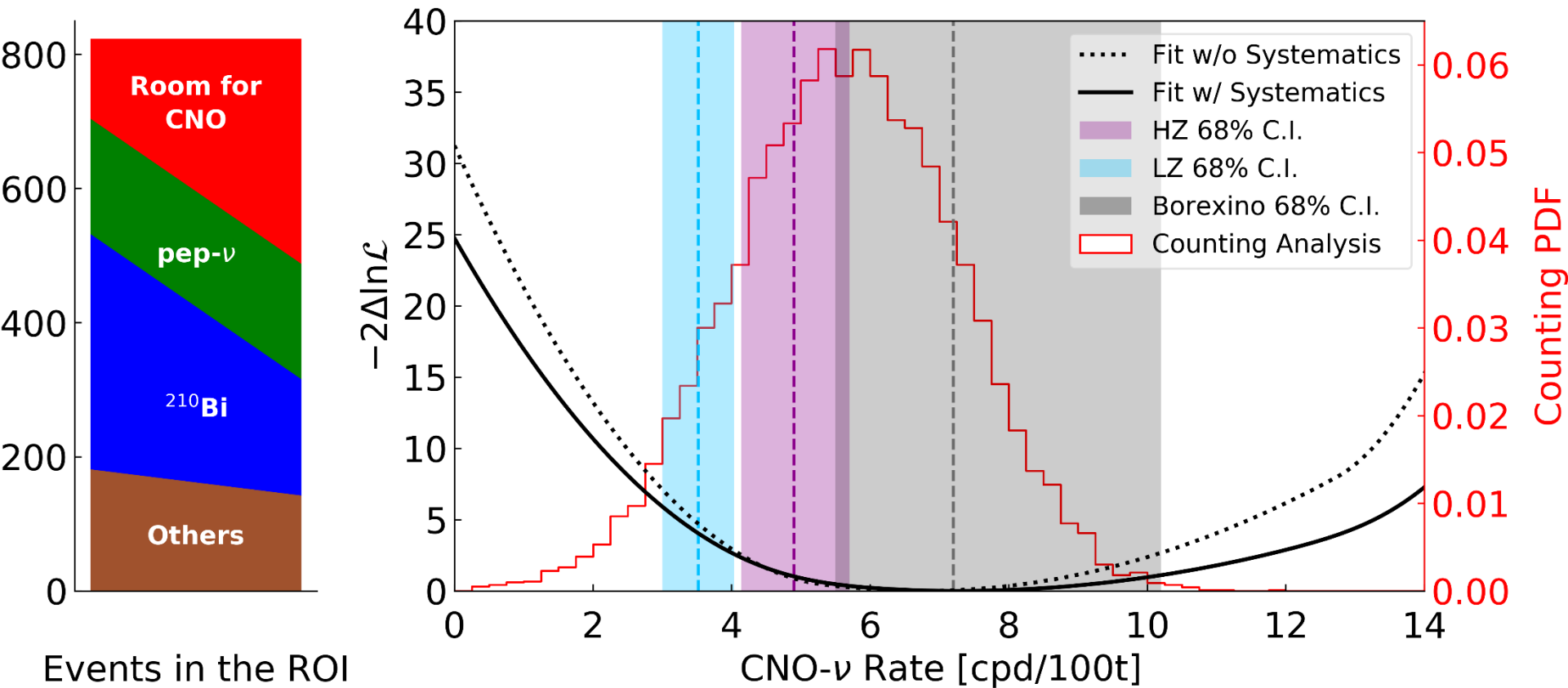
$$R_{\nu(\text{CNO})} = (5.6 \pm 1.6) \text{ cpd}/100t \quad [\sim 3.5 \sigma]$$

The multivariate fit fully exploits all the information contained in the data and substantially enhances the CNO significance

Consistent signal detection

Poster: "Counting analysis of Borexino Phase-III data for the detection of CNO solar neutrinos" Riccardo Biondi #93 session 2

Compendium of the results



The enduring Borexino quest of the CNO neutrinos has finally produced the first observation of the signal

Conclusion

The undeterred, several years long effort to thermally stabilize the detector has resulted in the first detection of **CNO** neutrinos by Borexino

Significance of the detection **5σ**

With this outcome Borexino has completely unraveled the two processes powering the Sun

the pp Chain and the **CNO Cycle**

Other posters: "Data quality and stability of the Borexino detector" Chiara Ghiano #189 session 2

"New limits on non-standard neutrino interaction parameters from Borexino data" A. Vishneva et al. #582 session 2

"The measurement of the geo-neutrino flux with the Borexino detector and its geophysical implications" Maxim Gromov and Sindhujha Kumaran #274 session 2

"Search for low-energy Borexino's signals correlated with gamma-ray bursts, solar flares and gravitational wave events" A. Derbin #57 session 4



Borexino Collaboration



UNIVERSITÀ
DEGLI STUDI
DI MILANO



Istituto Nazionale di Fisica Nucleare



PRINCETON
UNIVERSITY



UNIVERSITÀ DEGLI STUDI
DI GENOVA



NATIONAL RESEARCH CENTER
"KURCHATOV INSTITUTE"



St. Petersburg
Nuclear Physics Inst.



Technische Universität
München



Virginia Tech



JOHANNES GUTENBERG
UNIVERSITÄT MAINZ



SKOBELTSYN INSTITUTE OF
NUCLEAR PHYSICS
LOMONOSOV MOSCOW STATE
UNIVERSITY



Joint Institute for
Nuclear Research

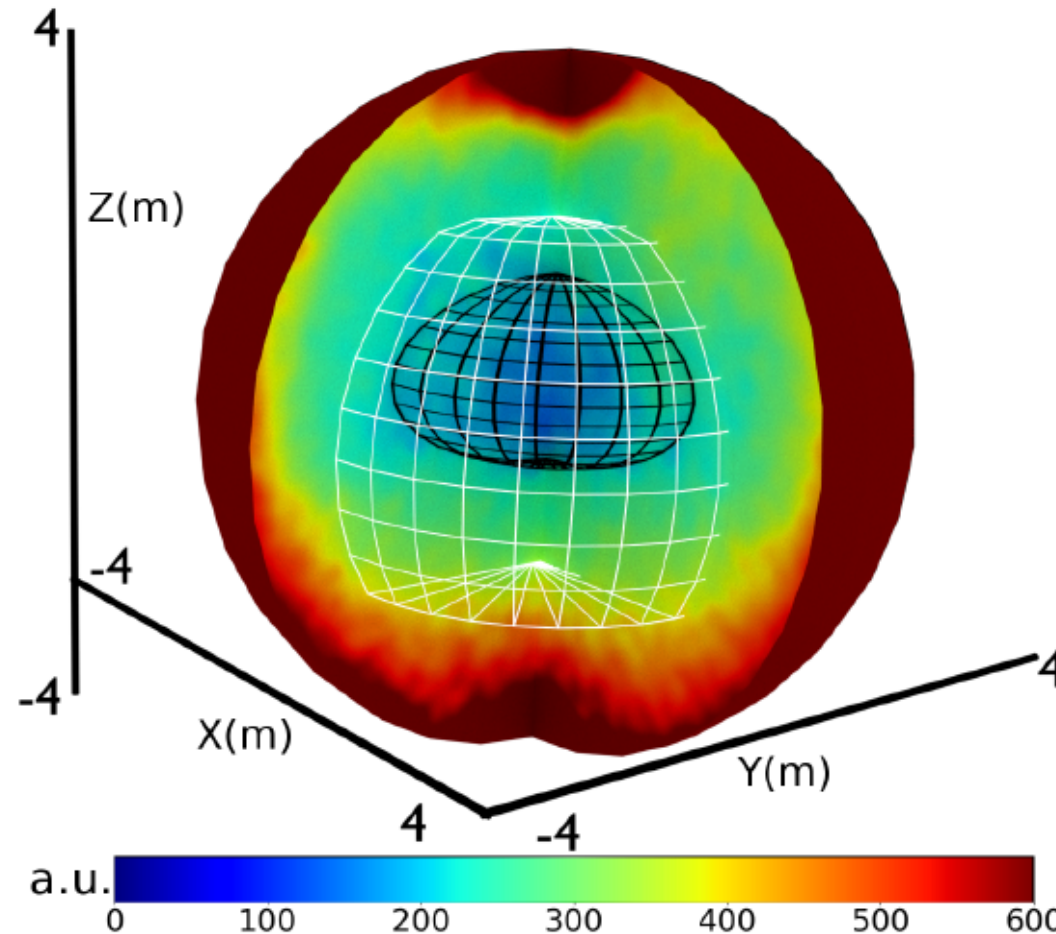


TECHNISCHE
UNIVERSITÄT
DRESDEN

RWTH AACHEN
UNIVERSITY

Back up

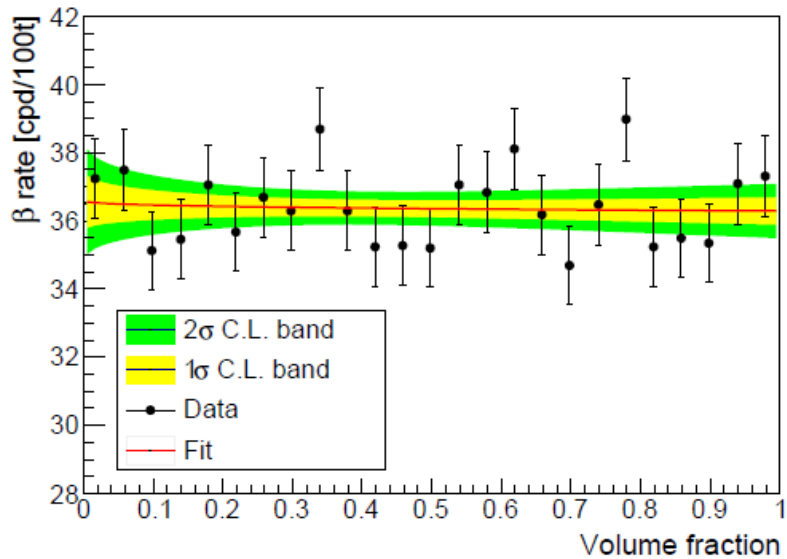
Low Polonium Field inside the scintillator



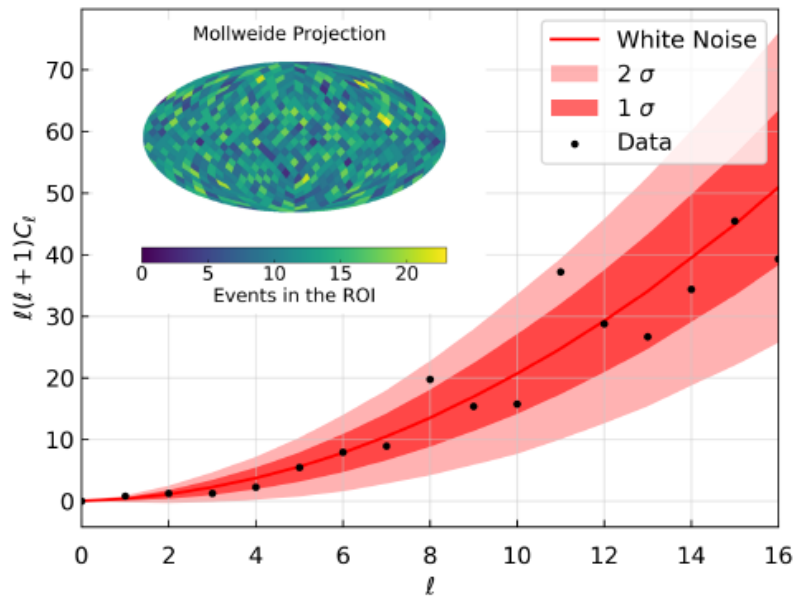
Three-dimensional view of the ^{210}Po activity inside the entire Inner Vessel - the innermost blueish region contains the LPoF (black grid) - the white grid is the software-defined Fiducial Volume

^{210}Bi spatial uniformity systematics angular and radial derivations

Angular Power Spectra



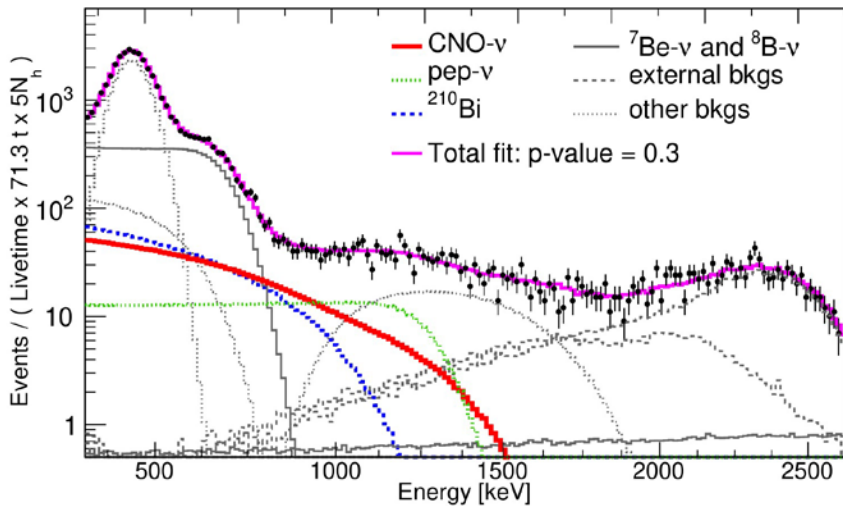
Linear fit performed over the variable r/r_0 where r_0 is the radius of the sphere surrounding the analysis fiducial volume
data are found compatible with a uniform distribution within 0.5 cpd/100t



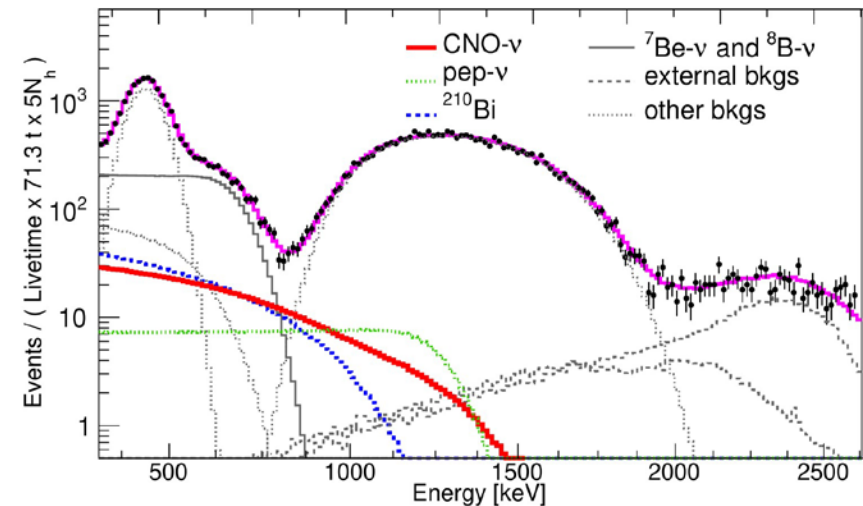
Angular spectral density of observed β events in the ^{210}Bi ROI (black points) compared with 10000 uniform event distributions from Monte Carlo simulations at one (dark pink) and two σ CL (pink)
data are found compatible with uniform distribution within the uncertainty of 0.59 cpd/100t - inset: angular distribution of the β rate in the ^{210}Bi ROI

The three distributions in the multivariate fit

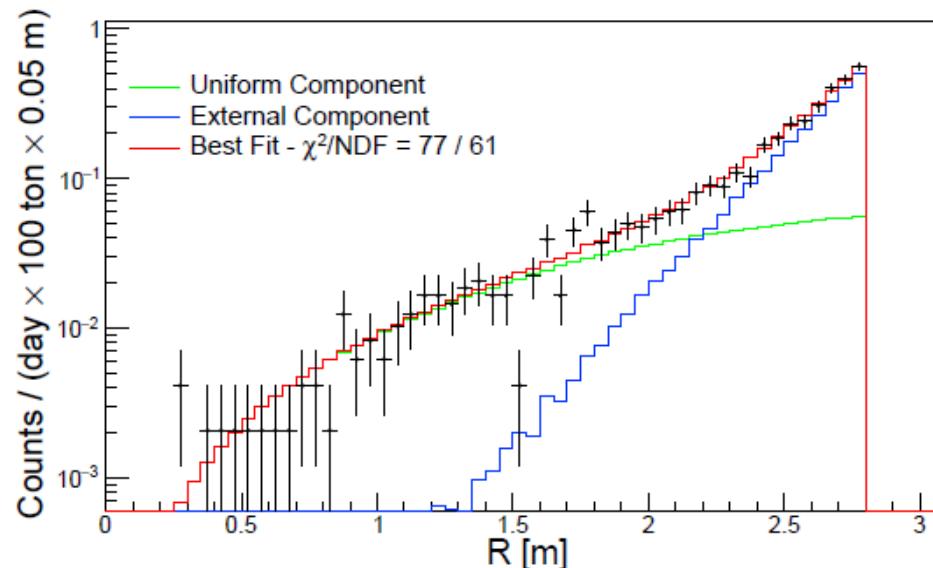
TFC-subtracted spectrum



TFC-tagged spectrum



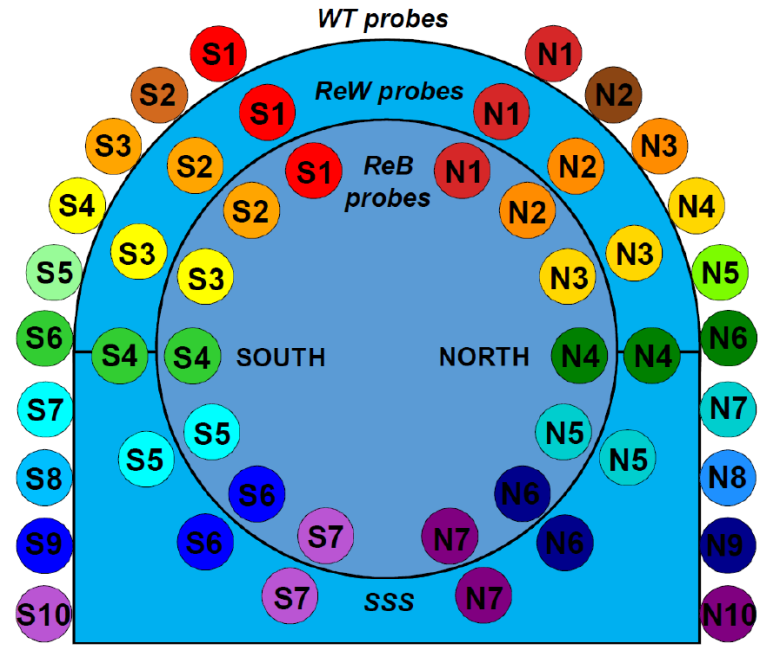
Radial distribution of events



Instrumentation of the detector for thermal stabilization and monitoring



Borexino Water Tank after the completion of the thermal insulation layer



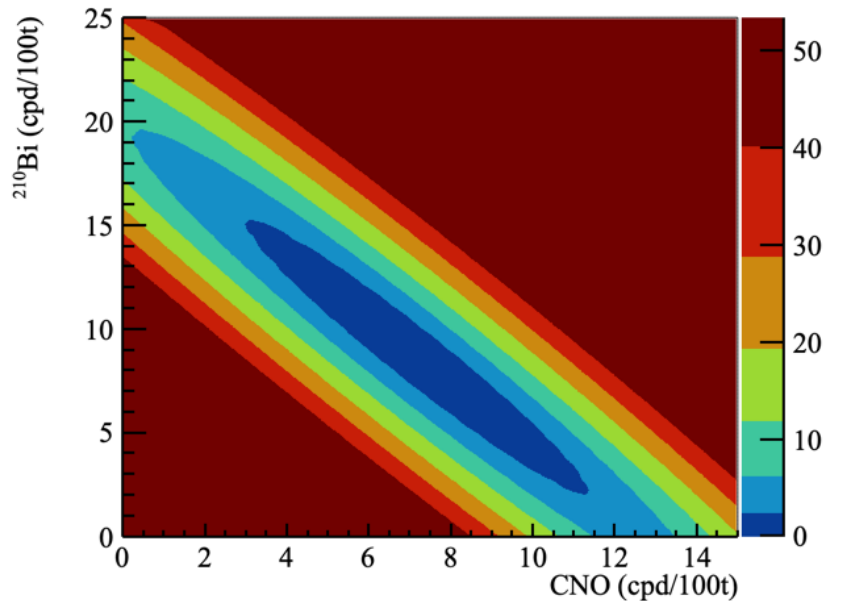
Distribution of temperature probes around and inside the Borexino detector

Table of solar ν fluxes with SSM HZ/LZ

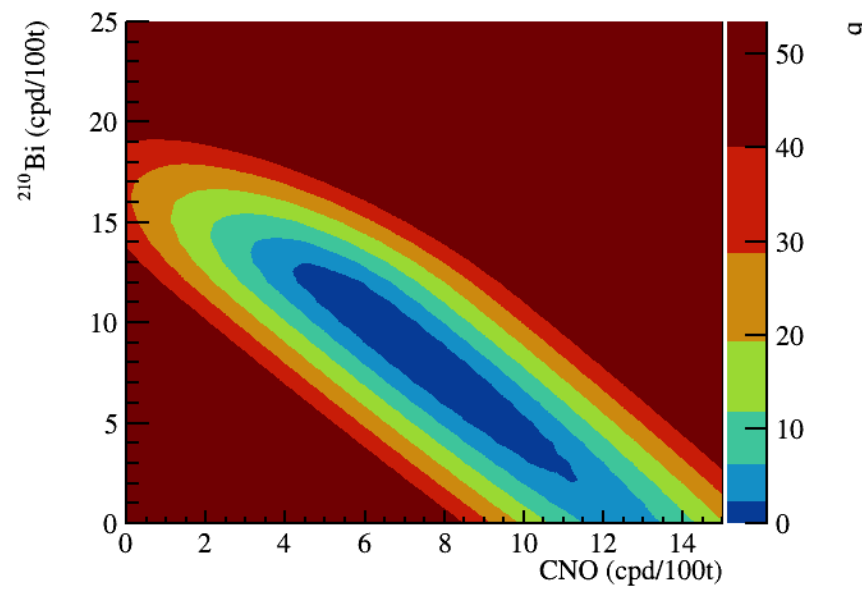
	GS98	AGSS09met	Obs
$\Phi(\text{pp})$	$5.98(1 \pm 0.006)$	$6.03(1 \pm 0.005)$	$5.971^{+0.037}_{-0.033}$
$\Phi(\text{pep})$	$1.44(1 \pm 0.01)$	$1.46(1 \pm 0.009)$	1.448 ± 0.013
$\Phi(\text{hep})$	$7.98(1 \pm 0.30)$	$8.25(1 \pm 0.30)$	19^{+12}_{-9}
$\Phi(^7\text{Be})$	$4.93(1 \pm 0.06)$	$4.50(1 \pm 0.06)$	$4.80^{+0.24}_{-0.22}$
$\Phi(^8\text{B})$	$5.46(1 \pm 0.12)$	$4.50(1 \pm 0.12)$	$5.16^{+0.13}_{-0.09}$
$\Phi(^{13}\text{N})$	$2.78(1 \pm 0.15)$	$2.04(1 \pm 0.14)$	≤ 13.7
$\Phi(^{15}\text{O})$	$2.05(1 \pm 0.17)$	$1.44(1 \pm 0.16)$	≤ 2.8
$\Phi(^{17}\text{F})$	$5.29(1 \pm 0.20)$	$3.26(1 \pm 0.18)$	≤ 85

Neutrino fluxes for the two HZ and LZ SSM as determined by J. Bergstrom et al., JHEP 03, p. 132 (2016) - the fluxes are given in units of 10^{10} (pp), 10^9 (^7Be), 10^8 (pep, ^{13}N , ^{15}O), 10^6 (^8B , ^{17}F), and 10^3 (hep) $\text{cm}^{-2} \text{s}^{-1}$

2D log-likelihood plots with respect to CNO and ^{210}Bi



Without ^{210}Bi constraint



With ^{210}Bi constraint

Intervals from the normalized likelihood

